



**VICTORIA UNIVERSITY**  
MELBOURNE AUSTRALIA

*Primary frequency control of a microgrid with integrated dynamic sectional droop and fuzzy based pitch angle control*

This is the Accepted version of the following publication

Datta, Ujjwal, Shi, Juan and Kalam, Akhtar (2019) Primary frequency control of a microgrid with integrated dynamic sectional droop and fuzzy based pitch angle control. *International Journal of Electrical Power and Energy Systems*, 111. pp. 248-259. ISSN 0142-0615

The publisher's official version can be found at  
<https://www.sciencedirect.com/science/article/pii/S0142061518338705>  
Note that access to this version may require subscription.

Downloaded from VU Research Repository <https://vuir.vu.edu.au/38368/>

# Primary frequency control of a microgrid with integrated dynamic sectional droop and fuzzy based pitch angle control

Ujjwal Datta<sup>a,\*</sup>, Juan Shi<sup>a</sup>, Akhtar Kalam<sup>a</sup>

<sup>a</sup>College of Engineering and Science, Victoria University, P.O. Box 14428, Victoria 8001, Melbourne, Australia

## Abstract

In a microgrid (MG), employing conventional fixed droop gain control of wind turbine for mimicking conventional generators may threaten grid stability. In this paper, an integrated control strategy of inertia emulation and dynamic sectional droop control for generating active power reference of the wind power system is presented to provide primary frequency control (PFC) services. The dynamic sectional droop is implemented with the fuzzy logic controller (FLC) regulated pitch angle control mechanism and compared with the conventional proportional-integral (PI) pitch angle control method in the isolated MG. Two different gain values are selected for developing the proposed sectional droop control which is based on the sensitivity of frequency deviation in comparison to the single fixed gain in conventional droop control. The maximum power margin of wind turbine is considered as 25% and 15% for a wind speed higher than (or equal to) the rated speed and lower than the rated speed, respectively. The effectiveness of the proposed method is investigated through Matlab/Simulink based real-time simulation studies. Simulation results demonstrate that the proposed sectional droop control provides superior performance than conventional fixed-gain method and achieves optimum frequency regulation at the rated wind speed and even for a wind speed lower than the rated wind speed.

*Keywords:* Dynamic sectional droop, primary frequency control, wind energy, PI controller, fuzzy logic controller

## 1. Introduction

The evolution in wind technology, reduction in renewable energy costs, renewable amiable government legislations on renewable energy have resulted in the upward trend of wind energy penetration in present-day power systems [1]. The doubly fed induction generator (DFIG) is one of the many wind energy technologies that is leading the path as a result of their dynamic potential of regulating active and reactive power and producing maximum power output [2, 3].

Inherently, wind speed defines the amount of wind turbine (WT) output and therefore bound to have variable output during their operation due to fluctuating wind speed. This fluctuating nature of WTs introduces new challenges to the power system stability and security, especially in a small isolated MG system. In order to maintain power balance, the base-load unit has to regulate its output accordingly and this results in additional stress on base-load power generation unit and affects its overall lifetime [4]. The DFIG operates in maximum power transfer mode when the wind speed is below rated value [5]. Pitch angle control regulates DFIG power near the rated power at the rated wind speed. As WTs do not provide inherent inertia support due to the employment of power electronics interface, the increased contribution of wind energy in the grid raises stability concern. In a grid-connected

mode, large synchronous generators take the responsibility to mitigate any temporary power imbalances. However, in a MG with renewable sources such facilities are very limited to obtain. Energy storage is found to be an equivalently alternative solution for providing temporary power imbalances [6]. Nevertheless, the imposed additional costs of storage facilities are still a valid argument from technical-economic perspective. Considering the economic challenges of storage system and mandatory inertia control regulating obligation, it is imperative that wind farm takes part in primary frequency control (PFC).

Many countries such as in UK, Ireland, Denmark, Canada, Netherlands and Germany already have mandatory power-frequency (P-f) regulation requirements for wind farms in order to be connected to the grid. This indicates that in industry, wind farms are required to provide (P-f) services to be a part of the grid. The grid codes requirement for power margin varies between countries. In UK, the required fixed P-f droop is between 3% to 5% for primary and secondary frequency control [7], whereas in Canada, Independent Electricity System Operator requires at least 10% boost in active power during frequency drop [8]. The Danish grid code requires a wind farm to respond in P-f upward and downward regulation within the 10% to 100% of wind farm capacity [9, 10]. The Irish grid (EirGrid) requires active power reduction to 15% [11] and TenneT, a transmission system operator (TSO) in Netherlands and the large part of Germany requires 25% reduction of the present generated active power during over-frequency periods [12]. A very limited

\*Corresponding author at: College of Engineering and Science, Victoria University, P.O. Box 14428, Victoria 8001, Melbourne, Australia. Tel.: +61 0470396067

Email address: [ujjwal.datta@live.vu.edu.au](mailto:ujjwal.datta@live.vu.edu.au) (Ujjwal Datta)

information is available on the actual P-f implementation and performance analysis by the wind turbine manufactures and TSO due to copyright issues and business policy. However, a field demonstration by General Electric (GE) shows that GE wind turbine can increase its power output by 5% to 10% during under-frequency events [13]. A field trial by the Australian Energy Market Operator in “Hornsedale Wind Farm 2” has considered 10% power margin for under-frequency events and this will further be explored in other wind farms as well [14].

In literature, a number of research works have suggested different control methods of emulating inertia by WT and scaling down instantaneous frequency fluctuations [7-17]. The authors in [15] demonstrated that WT significantly reduces the rate-of-change-of-frequency (ROCOF) when providing emulated inertia. Another study shows that the inertia emulation (IE) of WT results in lower frequency drop and faster recovery of rotor speed [16]. However, the study in [17] demonstrated that emulated inertia has little contribution in improving overall frequency response and may worsen the frequency performance rather than enhancing it. The IE can provide better frequency nadir than the droop control, nevertheless, droop control exhibits faster and higher frequency recovery value than the IE control [18]. On the other hand, droop control is found to be the outstanding alternative of IE in reducing frequency drop and ROCOF [19, 20]. In consideration of individual performance analysis, researchers have recommended the combined control of IE and droop control method for regulating the active power of WT and participating in PFC [21, 22]. The incorporated control method achieves exceptional performance in providing improved lower frequency excursion, faster frequency recovery, and lower steady-state error [23–25] in comparison to their respective control.

WT participates in PFC by reducing or increasing (within stored energy capacity) its power output during PFC. This energy regulation is achieved by operating the wind farm at a point other than the maximum power point. Many research works have proposed such deloaded operation of wind turbine through power [26] and torque [27] control. During the last decade, numerous control approaches have been presented to implement efficient pitch control [20-25]. Some of the studied control methods are proportional pitch control with pitch compensation to enhance DFIG performance [28], PI controller to enhance the stability of wind energy system in the case of contingencies [29], PID and non-linear  $H_{\infty}$  controllers to track the expected power output [30], FLC to smooth wind power fluctuations [31], Fuzzy-P and Fuzzy PID for controlling output power and achieving an optimal balance between power output and mechanical load [32]. However, the study in [33] argued that the pitch control is comparatively slow in response and therefore, the torque control is favored over pitch control [34]. Realizing the fact that torque provides faster response with limited control capacity and pitch angle shows slow response but has large torque control ability, coordinated control is suggested by many researchers [31-32]. The study in [35] revealed that the combined torque and pitch

control ensures stable and accurate control. In addition, the coordinated control of pitch control and the combined droop and inertia control with fixed gains shows better output response [36, 37]. Also, the study in [38] observed that torque droop achieves improved stability margin than the power droop. The study in [39] showed that the combined pitch control and IE effectively reduces frequency deviation and improves the frequency response. A coordinated FLC-energy storage (ES) is proposed in [40] for generating active power reference of DFIG in order to provide short-term frequency response. However, no ES is considered in this study for providing PFC services.

Number of researchers have identified the related concern of conventional linear droop gain and hence suggested variable droop gain schemes such as online tuning [22] with PI regulated pitch angle control to avoid possible instability phenomena. A dynamic droop gain, based on ROCOF scheme, is selected in [41] with the conventional pitch angle control to improve frequency nadir. The upper and lower droop values are chosen in [42] for implementing dynamic droop control along with the conventional PI pitch angle controller. A virtual inertia controller to generate active power reference and deloading PI pitch angle controller regulated dynamic power-frequency (P-f) droop is presented in [43] to provide inertial response and PFC functions, nonetheless, the droop gain is adjusted manually. A coordinated control of droop-inertia is proposed in [44] to provide PFC service in a MG. A time varying gains for droop and inertia control is proposed in [45] for frequency regulation in which droop gain is reduced with time. Nevertheless, in both studies [44, 45], no explicit information is available of the incorporated pitch angle control method. A time-dependent droop gain is proposed in [46] for frequency support. However, fixed time-dependent droop gain may not provide satisfactory performance in different operating conditions. Two different droop values are selected in [47] for the wind speed greater than or equal to the rated value and below the rated speed along with a PI pitch angle control for frequency control. All the earlier literatures [7-19, 27-39] on PFC of the wind power system lack the design of the combined governing of dynamic droop and inertia control for regulating active power reference of DFIG and FLC regulated pitch angle control. Moreover, a significant portion of the studies did not consider real time investigation on the performance analysis of the control methods.

Although PFC regulation through deloading is widely studied in the literature, the proposed sectional droop control with inertia control for generating power reference and FLC regulated pitch angle control is different in which the level of power margin for PFC is regulated based on the sensitivity of frequency variation. The real-time simulation is carried out to demonstrate the effectiveness of the proposed control method using OPAL-RT, a real time digital simulator (RTDS). The main contributions of this study are as follows:

- (1) A novel sectional droop control coordinated with emulated inertia technique is designed to provide PFC services in wind power system. The dynamic sectional droop control

is divided into two different regions based on P-f sensitivity; highly sensitive region for low-frequency deviation and less sensitive region for higher frequency deviation.

- (2) The performance of the sectional droop control is investigated with proportional-integral (PI) and FLC regulated pitch angle control.
- (3) The simulation is carried out in real-time using RTDS which can meticulously imitate the physical systems which carries a great value in term of efficacy analysis of the control approach.
- (4) Single and multiple DFIG units are taken into consideration in order to investigate the usefulness of the proposed control method in a simple and complex MG system.
- (5) Two separate power margins are adopted: a) 25% power margin considering the wind speed greater than or equal to the rated value and b) 15% power margin in view of wind speed below the rated value to avoid unwanted large oscillations.

The rest of the paper is arranged as follows: The discussion on conventional droop and inertia control schemes are presented in Section 2. Section 3 provides the detailed discussion on the proposed dynamic sectional droop control. The proposed FLC regulated pitch angle control is presented in Section 4. Section 5 briefly describes the wind turbine and the studied MG modeling. The results and analysis of Matlab/Simulink based real-time simulation studies and summary of the paper are presented in Section 6.

## 2. Conventional Droop and Inertial Control Schemes

By convention, grid-connected synchronous generators (SGs) generate/absorb temporary shortcomings between the generated and demanded power through inertia service by means of regulating stored kinetic energy. With the advent of sophisticated control mechanism of wind turbine, droop-inertia control method can be implemented in DFIG controller for emulating the behavior of SGs. To implement such inertial control, WTs need to be operated at a power point other than the maximum power point tracking (MPPT). Thus deloading creates proportionate power margin by regulating wind rotor speed above or below the rated speed for participating in frequency regulation. The IE in the case of contingencies can be written as in (1):

$$\Delta P_{IE} = K_{IE} \frac{d}{dt} \Delta f = 2H_G \frac{d}{dt} \Delta f \quad (1)$$

where,  $K_{IE}=2H_G$ ,  $H_G$  is the inertia gain,  $\Delta f$  is the frequency error between the grid and the reference frequency. The power reference generated from the droop and inertia control loop is added with the actual power reference of DFIG to provide the updated power reference to the rotor side converter of the DFIG control as shown in Fig. 1. The addition/reduction in wind power reference is determined by the sign of frequency error and the amplitude is calculated

according to (1) that defines the intensity of inertia participation by the DFIG. To avoid unnecessary operation for a small change, a deadband of  $\pm 0.05\text{Hz}$  is applied. The wind inertia gain is selected as  $0.2\text{pu}$ . The inertia response plays dominant role at the beginning of the contingencies but has less impact with the developing frequency variation. The droop control loop shows an effective contribution in regulating primary frequency followed by the large frequency variations. Therefore, droop control is added with the inertia loop to provide better frequency performance. The conventional droop control can be defined as in (2):

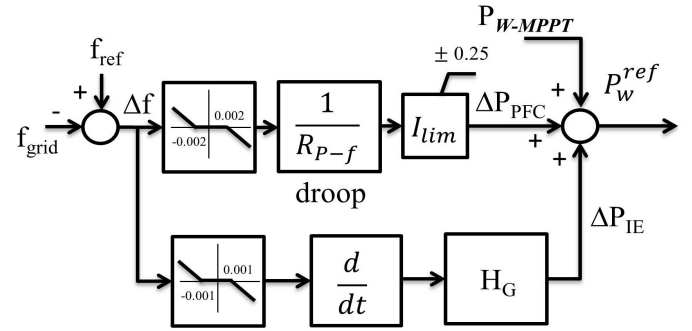


Fig. 1 Inertial and Conventional Droop Control

$$\Delta P_{PFC} = \frac{1}{R_{P-f}} \Delta f \quad (2)$$

where,  $R_{P-f}$  is the droop value. To accomplish the updated power reference ( $P_w^{ref}$ ) with the droop and inertia control loop, the generated power reference of PFC in (2) and IE in (1) are accumulated with the MPPT power reference ( $P_{W-MPPT}$ ) as shown in Fig. 1 and in (3):

$$P_w^{ref} = P_{W-MPPT} - \Delta P_{PFC} - \Delta P_{IE} \quad (3)$$

For a frequency higher than the rated, the values of  $\Delta P_{PFC}$  and  $\Delta P_{IE}$  are negative with respect to  $P_{W-MPPT}$  which indicates the power reduction of DFIG and vice versa. In order to represent 25% power margin during the frequency regulation, the value for droop gain is selected as 31.25 that defines the maximum power margin to be activated for a frequency deviation of 0.008pu, outside of the deadband boundary of 0.002pu. An intensity limit ( $I_{lim}$ ) is used at the droop control loop output to ensure a maximum power margin of 25% for frequency deviations beyond 0.008pu.

As droop controller has a dominant impact on the overall frequency performance, the fixed gain may bring out rapid acceleration/deceleration near the smaller frequency oscillations. Therefore, an alternative measure needs to be adopted to ensure smoother and stable frequency regulation.

## 3. The Proposed Sectional Droop Control Schemes

A high droop control gain (small R value) may provide better frequency regulation but choosing a small R value may

result in unexpected oscillations for low frequency deviations, mainly near the non-operating frequency boundary region. Hence selecting a small gain for smaller frequency deviation and large droop gain for higher frequency deviation is very crucial for frequency control. The sectional droop control is proposed for controlling EV charge/discharge in [48].

A dynamic sectional droop control is proposed to regulate the output of DFIG when participating in frequency regulation. This facilitates to obtain various levels of droop gain for the corresponding frequency deviation. The proposed dynamic droop control is shown in Fig. 2 which regulates droop gain in relation to the changes in frequency rather than wind speed as in [41, 42]. The dynamic droop control replaces the conventional droop control and added with the inertial control loop as shown in Fig. 1. The droop control gain is calculated with reference to the changes in frequency deviation ( $\Delta f$ ). When the frequency deviation stays within the deadband boundary between  $\Delta f_L$  and  $\Delta f_H$ ,  $\Delta f=0$  and also the associated power reference for PFC  $P_0 = 0$  as marked in red in Fig. 2. The same level of frequency deadband of  $\pm 100\text{Hz}$  is applied for activating sectional droop control. The sectional droop control is implemented by designing two different droop gains for low and high sensitive frequency region.

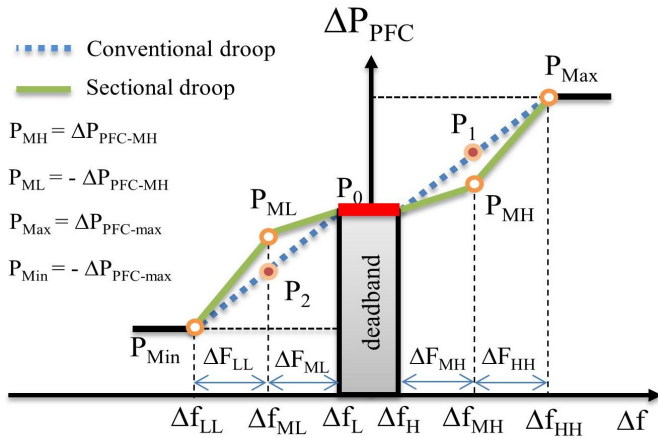


Fig. 2 The Proposed Conventional and Sectional Droop Control Strategy

The high sensitive region is designed to have reduced active power participation factor compared to the higher levels of participation rate for low sensitive region. The purpose is to scale down DFIG sharing for smaller changes in frequency. The region between  $\Delta f_{ML}$  (medium-low) and  $\Delta f_{MH}$  (medium-high) indicates the area of small frequency fluctuation and it is delineated as high sensitive region. Linear P-f droop with high droop gain in this region may result in large oscillations due to the physical inertia of WTs. To avoid any unexpected behavior, lower droop gain is selected in the high sensitive region. The maximum power references in this region are  $P_{ML}$  and  $P_{MH}$  instead of the conventional droop power references of  $P_2$  and  $P_1$ . Thus the lower intensity of DFIG can be ensured during the smaller changes in frequency and expected to have smoother frequency regulation with the proposed sectional droop control. The participation factor of

DFIG increases rapidly beyond the point of  $f_{ML}$  and  $f_{MH}$ .

The proposed dynamic sectional droop control can be mathematically expressed as in (4):

$$\Delta P_{PFC} = \begin{cases} P_{Max} & \text{if } \Delta f \geq \Delta f_{HH} \\ P_{MH} + P_{WTH} & \text{if } \Delta f_{MH} < \Delta f < \Delta f_{HH} \\ P_{WTMH} & \text{if } \Delta f_H < \Delta f < \Delta f_{MH} \\ 0 & \text{if } \Delta f_L \leq \Delta f \leq \Delta f_H \\ -P_{WTML} & \text{if } \Delta f_{ML} < \Delta f < \Delta f_L \\ -P_{ML} - P_{WTL} & \text{if } \Delta f_{LL} < \Delta f < \Delta f_{ML} \\ P_{Min} & \text{if } \Delta f \leq \Delta f_{LL} \end{cases} \quad (4)$$

The associated power coefficient values are:

$$\begin{aligned} P_{WTH} &= \frac{P_{Max} - P_{MH}}{\Delta f_{HH} - \Delta f_{MH}} (\Delta f_{HH}) \\ P_{WTMH} &= \frac{P_{MH}}{\Delta f_{MH}} (\Delta f_{MH}) \\ P_{WTML} &= \frac{P_{ML}}{\Delta f_{ML}} (\Delta f_{ML}) \\ P_{WTL} &= \frac{P_{Min} - P_{ML}}{\Delta f_{ML} - \Delta f_{LL}} (\Delta f_{LL}) \end{aligned} \quad (5)$$

At a frequency deviation of  $\Delta f_{HH}$  (high-high) and  $\Delta f_{LL}$  (low-low), the maximum power margin of DFIG ( $\Delta P_{Max}$  and  $\Delta P_{Min}$ ) is expected to be stimulated. The maximum participation factor of 25% by the DFIG is the same for the both droop control methods. The power references for PFC in high responsive positive and negative frequency zone are  $P_{WTMH}$  and  $P_{WTML}$ . The DFIG regulates its power output with respect to the changes in  $\Delta f$ . The proposed sectional and conventional droop parameters are plotted and shown in the Fig. 3. The studies in [42, 44] have considered 10-20% power margin for PFC whereas in [43] 28% deloading for PFC service has been selected. Considering the impact of variable wind speed on DFIG power output, two different levels of power margin is considered in this study. In this study, the maximum droop  $\Delta P_{PFC}=0.25\text{pu}$  (25%) is activated for a frequency deviation of  $\Delta f=0.008\text{pu}$  when the wind speed is at the rated value. The purpose of selecting 25% power margin is to ensure the availability of sufficient power margin that can regulate system frequency within  $\pm 1\%$  of the nominal value following the studied contingency events. The other limit of power margin is 15% when the wind speed is below the rated speed and the detailed discussion on variable power margin is presented in Section 5.3. In this study, the median sectional droop value of power is selected as  $\Delta P_{PFC}=0.056\text{pu}$  for a frequency deviation of  $\Delta f=0.004\text{pu}$ . This resembles a sectional droop gain of 14 compared to 31.25 in the case of conventional droop control for the high sensitive frequency region. In order to implement the proposed sectional droop control method, the deviation of frequency ranges for each section and associated power margin is selected on the basis of trial and error. It is worth noting that the optimal sizing of

power margin is not the focus of this paper. However, considering the importance of optimal sizing, an optimal tuning of P-f parameter for determining optimal power margin will get further attention in future study.

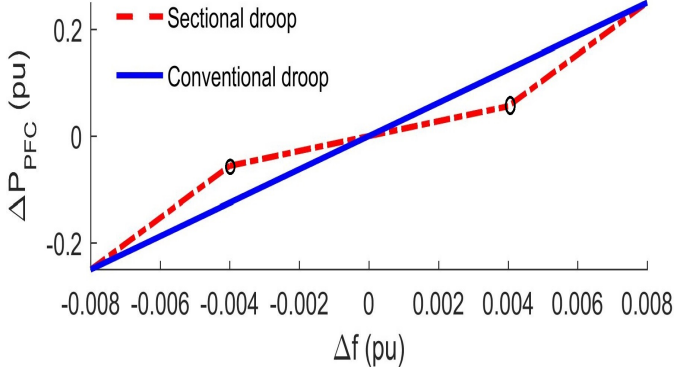


Fig. 3 Conventional and Sectional Droop with the Selected Parameters

When wind farm participates in PFC, the net power output may be reduced depending on the amount of energy exchange during an over-frequency/under-frequency event. Therefore, PFC may incur economic losses to the wind farm owner based on the amount of wind power output reduction compared to the amount of power supply to the grid during PFC services and the associated prices of exchanged energy. As such, a wide-range of techno-economic analysis is required to determine the financial outcome (economic gain/loss) of the provided frequency regulation service and validate the technical performance of PFC. However, this study is limited to the findings of PFC regulation only with the proposed control method. Hence, techno-economic analysis will get further attention in future studies.

## 4. Wind Energy Conversion System and Microgrid

### 4.1. Wind Turbine Modeling

The considered WT-type is DFIG for the studied MG and will be briefly discussed in this subsection. The mechanical power of the turbine can be written as in (6)

$$P_c = 0.5 \rho A C_p(\lambda, \beta) v_w^3 \quad (6)$$

where  $C_p$  is the power coefficient and a function of  $\lambda$  which is the tip speed ratio and  $\beta$  is the pitch angle,  $\rho$  is the air density,  $A$  is the turbine blade's sweep area.

The maximum power of DFIG is delineated by the power conversion coefficient  $C_p$  given that the incoming wind speed is constant. The maximum power, at a given wind speed, can be attained by coordinating the rotor speed reference through optimum tip speed ratio at a constant pitch angle. In normal operation, DFIG is operated at MPPT to extract maximum power. Nevertheless, DFIG must be forced to a deloaded point for participating in PFC.

The stored kinetic energy for PFC can be facilitated by various methods. Variable wind rotor speed is one of the many

suggested methods. The DFIG provides variable power output by varying rotor speed and creating temporary power margin. Therefore, by incorporating an additional control loop in DFIG controller, the DFIG can be designed to participate in PFC service. The proposed PFC strategy consists of the combined sectional droop control and FLC based pitch angle control.

### 4.2. Pitch Angle Control with Conventional PI

In this subsection, a brief discussion on the conventional PI regulated pitch angle control is provided. The turbine blade is governed by the pitch angle control for securing the DFIG from mechanical damages by restraining the power output of DFIG at the wind speeds above the rated speed. The traditional PI pitch angle controller along with pitch compensation to regulate the rated power output of WT is illustrated in Fig. 4. The pitch angle  $\beta_{ref}$  is normally positioned to zero to activate MPPT and produce maximum power in the course of a wind speed below the rated speed. In other conditions, the pitch angle control is activated for regulating the generated power or rotor speed to the rated value. The pitch angle control loop comprises PI regulator and pitch servomechanism as shown in Fig. 4. The time constant of pitch servo  $\tau_1$  defines the dynamic characteristics of the servo of the pitch angle control. As pitch servo system generally cannot respond quickly, a value of 0.25s is chosen for the pitch servo time constant. The dynamic nature of the pitch servo is constrained by the maximum and minimum pitch rate ( $d\beta/dt$ ). The pitch compensation is added to the new pitch rate. The updated pitch is subjected to the maximum ( $\beta_{max}$ ) and minimum ( $\beta_{min}$ ) pitch angles. The pitch angle passes through a first-order filter with a time constant of  $\tau_2=0.012s$  to generate pitch angle reference  $\beta_{ref}$ .

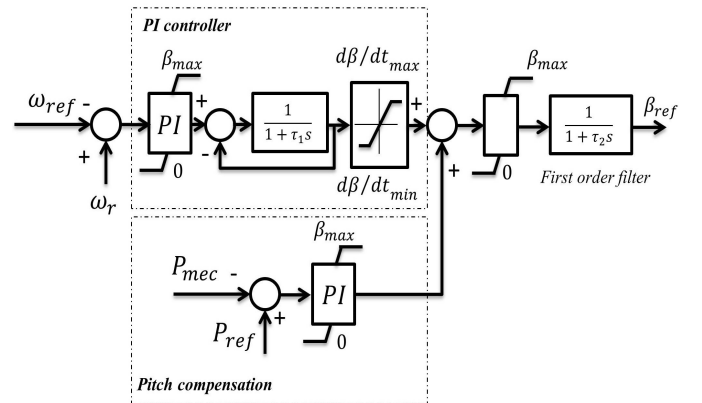


Fig. 4 The block diagram of conventional PI regulated pitch angle control

### 4.3. Pitch Angle Control with Fuzzy Logic

The detailed discussion on the proposed FLC based pitch angle control is presented in this subsection. The proposed FLC pitch angle control block diagram is shown in Fig. 5 which will be used to replace the PI controller shown in Fig. 4. The pitch angle reference at FLC output is determined by the fuzzified inputs, a set of rules (IF-THEN rules), the output

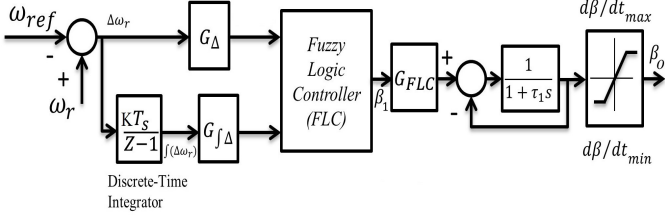


Fig. 5 The block diagram of FLC pitch angle control

from the FLC is obtained via Sugeno inference mechanism and then the output signal is obtained via de-fuzzification process.

To implement the control method, the deviation between the generator rotor speed and the reference value ( $\Delta\omega_r$ ) and the variation of the integration of rotor speed error ( $\int \Delta\omega_r$ ) are taken as inputs to the FLC. The inputs can be defined as shown in (7) and (8):

$$\Delta\omega_r(n) = \omega_r(n) - \omega_{ref}(n) \quad (7)$$

$$\int \Delta\omega_r(n) = \int \Delta\omega_r(n-1) + T_s \Delta\omega_r(n-1) \quad (8)$$

The pitch angle signal  $\beta_1$  is considered as FLC output. The variation of rotor speed deviation can be calculated by (8) according to the Forward Euler integrator method. The value of input scaling factors are the same as in PI controller i.e.  $G_\Delta=3$  and  $G_{f\Delta}=0.6$ . The Gaussian-type membership functions are used for the FLC inputs whereas the FLC output membership functions are singletons as shown in Fig. 6. In fuzzy logic control system, the input membership functions act as a means converting a crisp set of input signals to a fuzzy set using fuzzy linguistic variables whereas the output membership functions are needed for producing crisp output. A large number of membership functions for inputs and output will result in a large set of fuzzy rule table which can be computational intensive when implementing the fuzzy controller. However, a small number of membership functions for the inputs and output may result in undesirable controller performance. The earlier studies of FLC in [31, 52, 53] have considered 7 membership functions for both inputs and output. Hence, 7 membership functions are selected for FLC control in this study. The linguistic values are designated as Negative Big(NB), Negative Medium (NM), Negative Small (NS), Zero(ZE), Positive Small (PS), Positive Medium(PM), Positive Big(PB). The experience and knowledge-based approach is chosen to derive the set of rules for the FLC. The fuzzy rules formulation for inputs to the output can be expressed as in (9):

$$RL_k : \begin{cases} \text{IF } \Delta\omega_r(n) \text{ is } X_k \text{ and } \int \Delta\omega_r(n) \text{ is } Y_k \\ \text{THEN } \beta_o \text{ is } Z_k \end{cases} \quad (9)$$

where, fuzzy subsets are denoted by  $X_k$ ,  $Y_k$  respectively and  $Z_k$  is the singleton type output. The fuzzy rules with two inputs and 7x7 linguistic values for the inputs are given in Table 1.

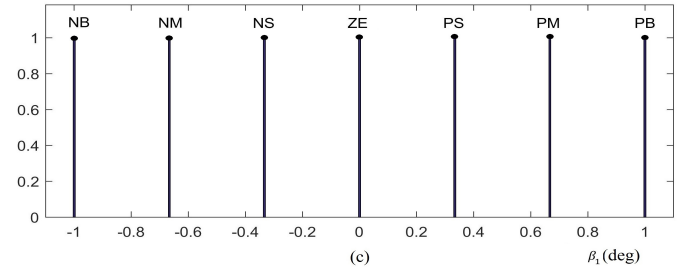
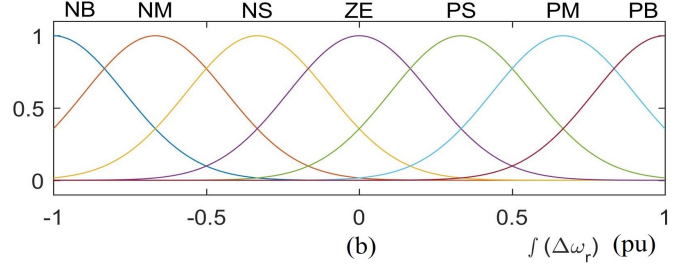
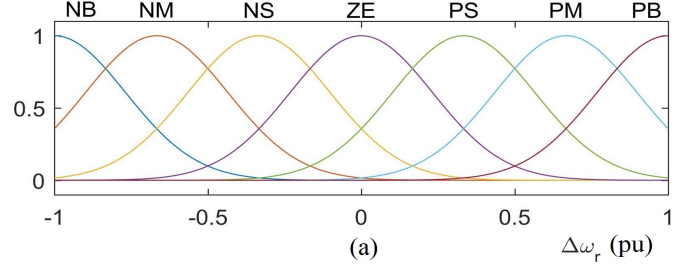


Fig. 6 Proposed FLC membership function for (a) wind generator rotor speed error (b) the integration of rotor speed error (c) pitch angle reference at FLC output

Table 1 FLC rules

$\int \Delta\omega_r$	NB	NM	NS	ZE	PS	PM	PB
NB	NB	NB	NB	NB	NM	NS	ZE
NM	NB	NB	NB	NM	NS	ZE	PS
NS	NB	NB	NM	NS	ZE	PS	PM
ZE	NB	NM	NS	ZE	PS	PM	PB
PS	NM	NS	ZE	PS	PM	PB	PB
PM	NS	ZE	PS	PM	PB	PB	PB
PB	ZE	PS	PM	PB	PB	PB	PB

The Sugeno type FLC is enforced in this paper. The pitch angle output  $\beta_1$  is calculated as in (10)

$$\beta_1(n) = \frac{\sum_{k=1}^N W_k Z_k}{\sum_{k=1}^N W_k} \quad (10)$$

where, N denotes the total rules number,  $W_k$  is the rule weighting factor obtained from processing the IF part of the rules. The final pitch angle reference from FLC is calculated as  $\beta_1$ . The constant values are selected for the various scaling factors ( $G_\Delta=3$ ,  $G_{f\Delta}=0.6$ ,  $G_{FLC}=2$ ) in the FLC.

Fuzzy logic controller (FLC) is utilized to regulate pitch angle control whereas the multi-gain droop control is included

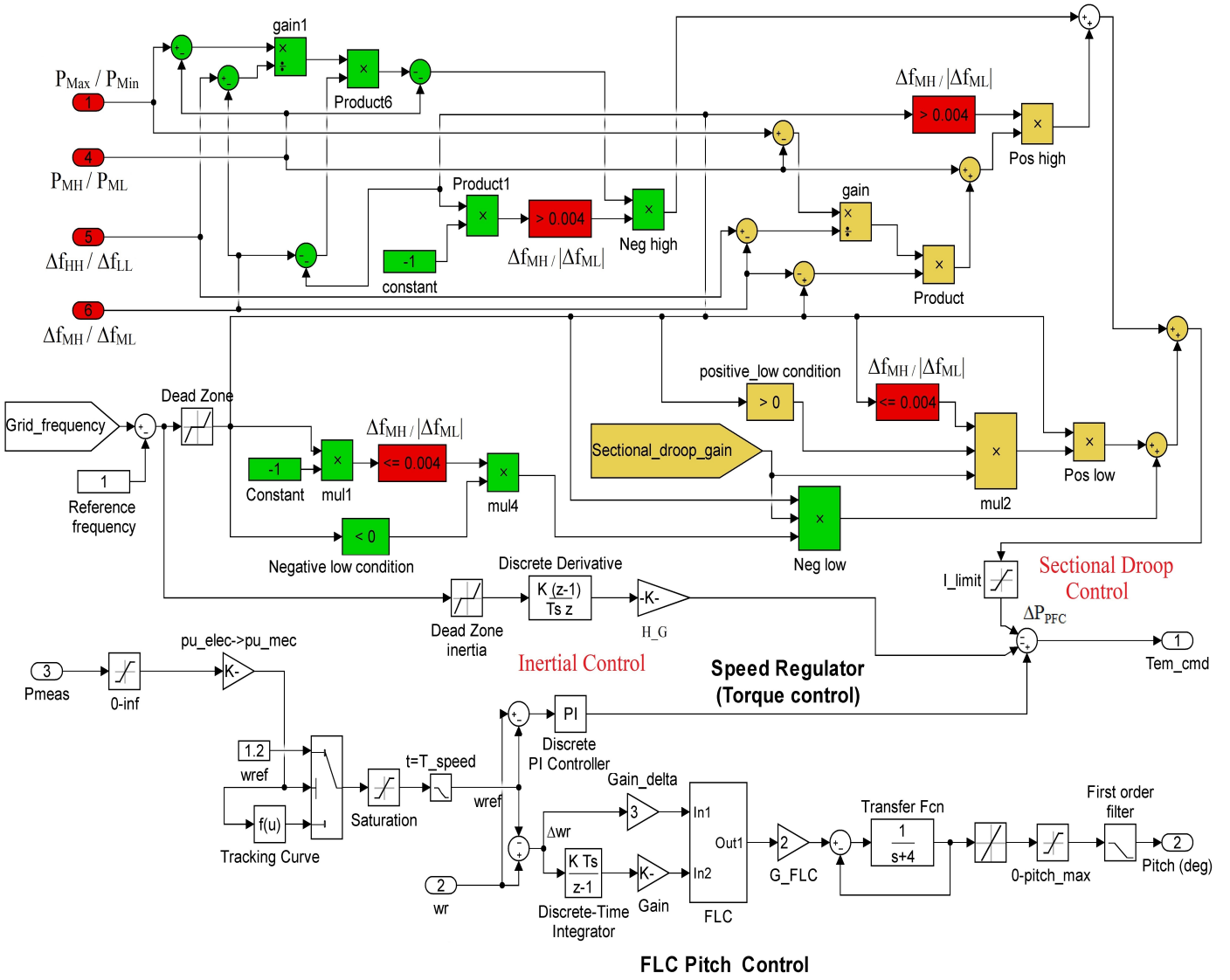


Fig. 7 The block diagram of the proposed FLC pitch angle control and sectional droop controller of DFIG

in the torque control signal of DFIG to regulate DFIG active power according to P-f characteristics defined by the droop controller gains. Hence, the total control diagram of DFIG pitch angle control with FLC and PFC control combined with the proposed sectional droop controller and inertia control is shown in Fig. 7. The droop parameters can be tuned by varying the value of maximum/minimum power margin ( $P_{max}/P_{min}$ ), frequency deviation ( $\Delta f_{HH}/\Delta f_{LL}$ ) and the value of median frequency deviation ( $\Delta f_{MH}/\Delta f_{ML}$ ) as shown in Fig. 7.

#### 4.4. Description of the Microgrid

A small isolated MG of 50Hz is used in this study as shown in Fig. 8. A 40MW synchronous generator (SG) and a 10.5MW aggregated wind farm are the power sources in the MG. The connected load at Load A is 25.8MW and 4MVAR and at Load B is 20.5MW and 5MVAR. The wind farm is located 10kms away from the load center and integrated to the MG at Bus 2. The inertia constants of SG and wind farm are

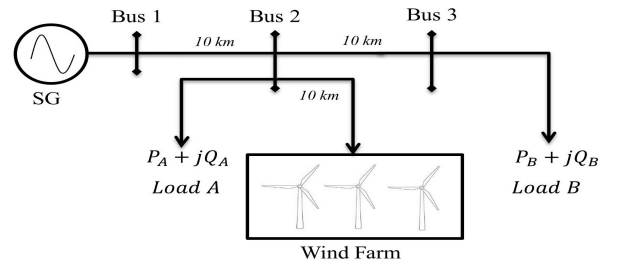


Fig. 8 Block diagram of the studied Microgrid

6.175s and 4.32s, respectively. In a MG, conventional SG may fail to provide sufficient frequency assistance as the penetration of low inertial wind energy increases. Therefore, it is very crucial that wind farm participates in PFC to ensure better frequency response in the case of grid contingencies. The nominal wind rotor speed is 1.2 pu at the rated wind speed

of 15m/s with an operating range of 0.7-1.3pu. The rated power is 10.5MW at a wind speed of 15m/s. The 6<sup>th</sup> order machine model is used for the SG combined with IEEE type 1 synchronous machine voltage regulator, hydraulic turbine and proportional-integral-derivative (PID) governor system.

## 5. Case Studies and Discussion

To verify the suggested control approaches, Matlab/Simulink studies have been conducted in a small isolated MG power system described in the previous section. The OPAL-RT based real-time simulation (RT-LAB) is performed to assess the comparative performance of the suggested control strategy. RTDS is capable of solving equations fast enough that practically can imitate the physical systems and widely used to design and test power system control strategy [49, 50]. Three different simulation studies have been performed and discussed in this section.

The first and second scenarios consider the load event and wind speed variation with rated wind speed. The wind speed below the rated value is considered in the last case study. The control strategies are given the following acronyms: conventional droop PI pitch control (CDPP), conventional droop fuzzy pitch control (CDFP), sectional droop PI pitch control (SDPP) and sectional droop fuzzy pitch control (SDFP).

### 5.1. Effects of Load Event

A momentary 5MW load increase at Load A is applied between 1-1.45s. In response to the temporary load event, the frequency outcome with the conventional and the proposed control approaches are analysed and comparative performances of DFIG for PFC are illustrated in Fig. 9. When the wind speed is at the rated speed, the value of  $I_{lim}$  is 0.25pu.

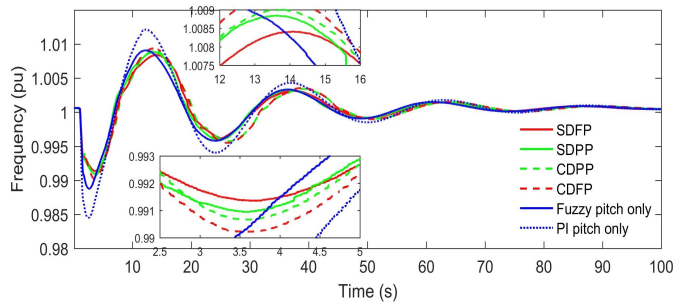


Fig. 9 The frequency output of synchronous generator with the load event

The dynamic outcome of the frequency response is illustrated in Fig. 9. The temporary load increase event increases frequency deviation ( $\Delta f$ ) from the initial zero value. The increased ( $\Delta f$ ) beyond the allowed band-activates the PFC feature of DFIG, forcing DFIG to shift its operation at a point other than the MPPT generation. It can be observed that without any PFC service (with fuzzy (49.44Hz) or PI (49.225Hz) pitch control only), the grid frequency experiences the highest drop in grid frequency resulted from the temporary

increased load event as shown in Table 2. In addition, Table 2 also reveals that even without the IR/PFC service, the proposed FLC yields better frequency response in terms of maximum ( $f_{max}$ ) and minimum frequency ( $f_{min}$ ) excursion than the PI pitch angle control. On the contrary, the proposed SDFP achieves the lowest frequency drop (49.575Hz) and rise (50.42Hz) and hence possesses the best performance in regulating frequency with PFC service. A closer examination of the frequency variation as shown in Fig. 9, at the beginning of the disturbance and in Table 2, clearly reveals the corresponding effectiveness of the proposed sectional droop control in comparison to the conventional droop control with both types of pitch angle controllers. FLC provides better result due to the fact that FLC does not change abruptly and operate according to the membership function and control cycle. This offers better regulation capability in non-linear environment compared to linear PI control and may not perform satisfactorily with the changing situation.

Table 2 The comparative analysis of frequency deviation with load increase event

Control method	$f_{min}(Hz)$	$f_{max}(Hz)$
SDFP	49.575	50.42
SDPP	49.55	50.44
CDFP	49.51	50.47
CDPP	49.535	50.445
Fuzzy pitch only	49.44	50.45
PI pitch only	49.225	50.6

According to Fig. 10, as anticipated, the variation in wind rotor speed is at the minimum value without any PFC services. When DFIG participates in PFC, DFIG creates temporary power margin by under-speeding and over-speeding. Referring to Fig. 10, it can be observed that the proposed sectional droop control with fuzzy pitch control handles the frequency response more smoothly than the other methods. The proposed control approach makes it happen by reducing the level of intensity near the edges of the low-frequency region. Therefore, as expected, SDFP exhibits better power regulation of wind farm while participating in PFC as shown in Fig. 11.

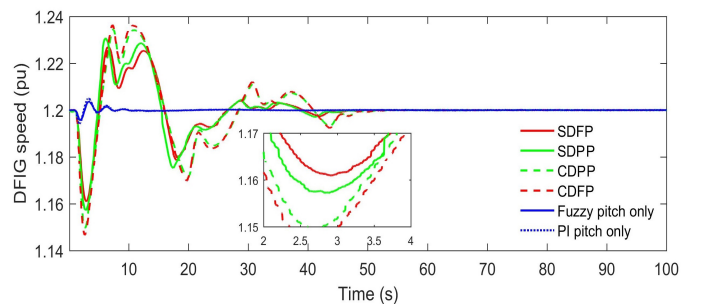


Fig. 10 DFIG rotor speed with load event

The P-f relationship with the conventional droop control settings (CDPP, CDFP) results in greater oscillations in pitch angle as shown in Fig. 12 and this phenomena can be seen in

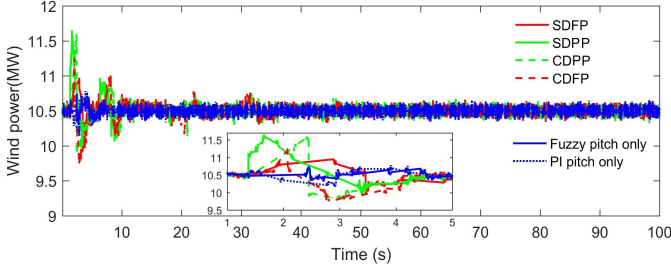


Fig. 11 The power output of wind farm with load event

the frequency outcome having larger oscillations. The proposed SDFP contributes further in regulating the frequency response of the grid more smoothly and demonstrates reduced frequency rise and fall following the temporary load increased event. The above analysis on DFIG dynamics reveals that the FLC pitch control performs better than the PI regulated pitch control. Also, the proposed sectional droop control substantiates its effectiveness compared to the conventional droop control setting.

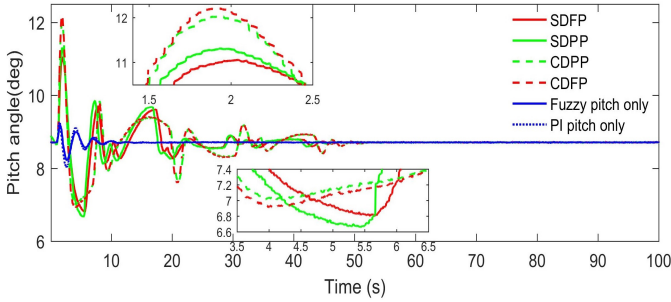


Fig. 12 The responses of DFIG pitch angle with different control approaches

### 5.2. Changes in wind speed

The frequency variation and DFIG response is further investigated in the event of wind speed variation. A series of step changes in wind speeds are applied; decreasing wind speed to 13m/s from 15m/s at  $t=1s$ , then increasing from 13m/s to 15m/s at  $t=3s$ , again increasing from 15m/s to 17m/s at  $t=5s$  and finally decreasing to 15m/s at  $t=8s$ . The comparative performances of the proposed and conventional droop control approaches are illustrated in Fig. 13 and in

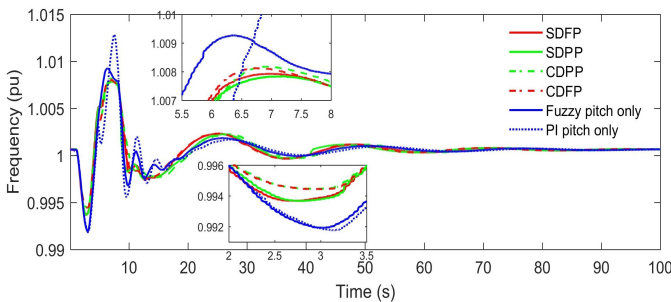


Fig. 13 The frequency output of the generator with the variation in wind speed

Table 3. Without any PFC service, large frequency oscillations are visible following the wind speed changes. Nevertheless, without PFC fuzzy pitch control contributes in better frequency regulation in comparison to PI pitch angle control as in the previous load event case. DFIG in PFC mode considerably reduces the frequency oscillations. Despite the fact that conventional droop control maintains slightly lower frequency drop than the sectional droop control, but, the sectional droop control manifests better outcome during the rise of frequency. In regard to the relative performance of individual pitch controller, both controllers with the sectional and conventional droop control settings show almost similar outcome in this case.

Table 3 The comparative analysis of frequency deviation with wind speed variation

Control method	$f_{min}(Hz)$	$f_{max}(Hz)$
SDFP	49.685	50.39
SDPP	49.685	50.395
CDFP	49.72	50.405
CDPP	49.72	50.41
Fuzzy pitch only	49.6	50.45
PI pitch only	49.59	50.6

Fig. 14 illustrates the superior performance of sectional droop control over conventional droop control. The conventional droop control incurs lower rotor speed variation during the fall of the frequency with reduced wind speed at  $t=1s$  that results in the lowest drop in grid frequency. On the contrary, when the wind speed is increased to 15m/s, the conventional droop control acquires greater power margin and this results higher frequency rise than the sectional droop control. The wind farm power output as illustrated in Fig. 15 shows the individual controller performance while participating in PFC.

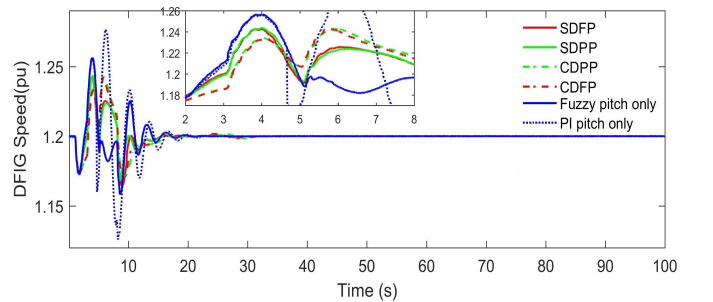


Fig. 14 DFIG rotor speed response in PFC with wind speed variation

### 5.3. Effects of Wind speed below the rated speed

The pitch angle control is set to zero when the WT operates at a wind speed below the rated speed to produce the maximum power at WT output. Hence, the efficacy of the proposed sectional droop control and the intensity of DFIG participation factor in PFC can be further explored in this case.

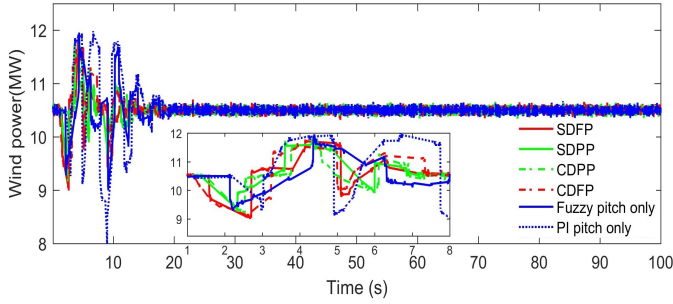


Fig. 15 Wind farm power output

The wind speed varies from 10m/s and the wind farm is producing 6MW power at the steady-state condition. The wind variation event as 10m/s to 9m/s at  $t=1$ s, then 9m/s to 10m/s at  $t=3$ s, next 10m/s to 11m/s at  $t=5$ s and finally reduces to 10m/s at  $t=8$ s.

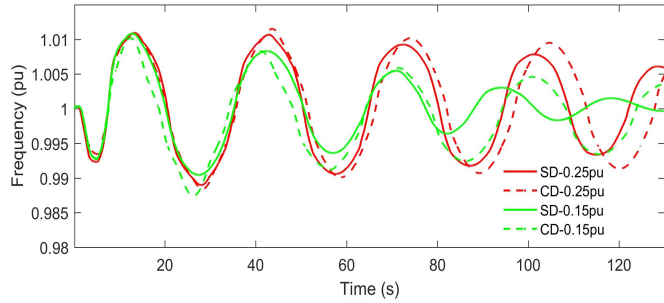


Fig. 16 The frequency outcome with variable power margin and wind speeds

The frequency output illustrated in Fig. 16 shows that with the applied wind speed variation event and below the rated speed the grid frequency experiences a continuous large oscillation for the power margin of 25%. This limitation arises considering the physical inertia of wind turbine and with the same amount of power margin for PFC, DFIG encounters large acceleration/deceleration. Nevertheless, sectional droop control exhibits decaying frequency oscillations at a faster rate than the conventional droop control. However, to avoid large power margin during the wind speed lower than the rated value, an additional intensity limit of WT power margin is adopted in this study. The adoption of the additional power margin is explained in Fig. 17. The limit of power margin is selected as 0.25pu when the wind speed is of rated value. If the wind speed is below the rated speed ( $<11$ m/s), the maximum power margin for PFC changes to 0.15pu.

The simulation results with the coordinated power margin at different wind speed in Fig. 16 manifests that with lower power margin frequency oscillations reduce significantly for the same wind speed variation. In addition, the proposed sectional droop control damps the frequency oscillation faster than the conventional droop control. This implies the outstanding accomplishment of the proposed sectional droop control strategy. On the other hand, for the similar load event as in Section 5.1 the frequency output as shown in Fig. 18 reveals that conventional droop control fails to stabilize grid

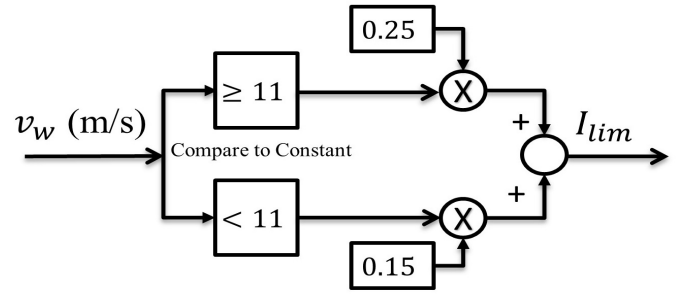


Fig. 17 The regulation of power margin intensity at various wind speed

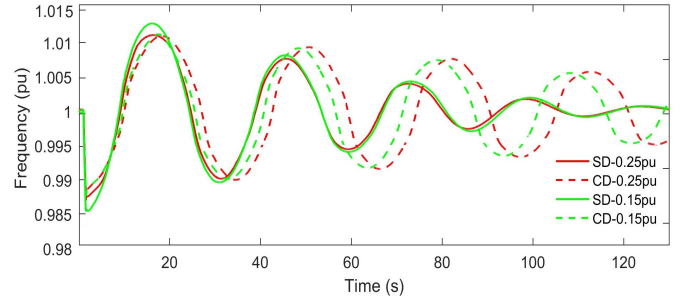


Fig. 18 The frequency outcome with variable power margin and load event

frequency regardless of the power margin level. On the contrary, sectional droop control possesses lowest drop and highest rise in frequency at the initial stage of the contingency. However, it can be observed that in terms of long operation time the sectional droop control effectively damps out oscillations and stabilizes the frequency at a faster rate for both power margins.

Table 4 The comparative analysis of frequency deviation with wind speed below the rated value

Power margin (right)		0.25pu		0.15pu	
Event (bottom)	frequency (Hz)	SD	CD	SD	CD
Wind speed variation	$f_{min}$	49.38	49.41	49.6	49.375
	$f_{max}$	50.55	50.57	50.55	50.51
Load decrease event	$f_{min}$	49.36	49.44	49.255	49.44
	$f_{max}$	50.551	50.551	50.6	50.551

The comparative frequency performances of the sectional and conventional droop controls are illustrated in Table 4. This analysis validates the remarkable performance of the proposed sectional droop control compared to the conventional droop control approaches during variable operating wind speed.

#### 5.4. Complex MG with multiple DFIG in PFC regulation

In order to further validate the efficacy of the proposed sectional droop control gain, a complex MG with extended load and wind generation units are considered as shown in Fig. 19, in which two DFIG based wind farms are taken into consideration. The rated power output of wind farms A and B are 10.5MW, individually. The wind farm B is located 10km away from wind farm A. Both wind farms are regulated with

the same control parameter settings for frequency regulation and other network parameters remain the same as in the previous MG network.

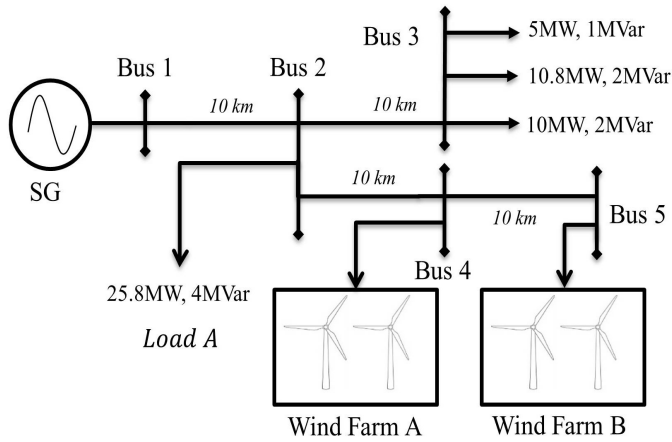


Fig. 19 The complex network with multiple DFIG based WT farm

A temporary 5MW load decrease at load A is applied for the duration of 1-1.5s and the dynamic frequency performances of the network with different controllers are presented in Fig. 20. It can be seen that the sectional and conventional droop with FLC regulated pitch angle control demonstrate improved oscillation damping compared to their corresponding conventional PI regulated approaches. In addition, the proposed sectional droop controller illustrates superior performance than the conventional droop control for both pitch angle controllers in terms of maximum and minimum frequency deviation as summarized in Table 5. Sectional droop possesses smaller frequency rise following the load decrease event and higher frequency nadir value during oscillation damping. Table 5 also reveals that, in the case of PI regulated pitch angle control, sectional droop control exhibits reduced frequency deviation compared to conventional droop control which validates the efficacy of the proposed sectional droop control than the conventional linear droop regardless of the types of pitch angle controller.

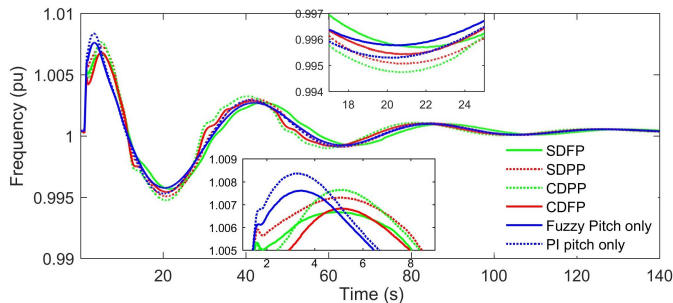


Fig. 20 The frequency outcome with multiple DFIGs in PFC regulation

The DFIG rotor speed of wind farm A is shown in Fig. 21. The sectional droop shows optimal rotor speed deviation following the load contingency events which explains the optimal frequency deviation of the proposed sectional droop.

Table 5 The comparative analysis of frequency deviation with load increase event in a complex MG

Control method	$f_{min}(Hz)$	$f_{max}(Hz)$
SDFP	49.785	50.33
SDPP	49.755	50.365
CDFP	49.77	50.34
CDPP	49.735	50.38
Fuzzy pitch only	49.79	50.38
PI pitch only	49.765	50.42

As both wind farms are configured with the same control parameter settings, rotor speed deviations are very similar for DFIG at wind farm B.

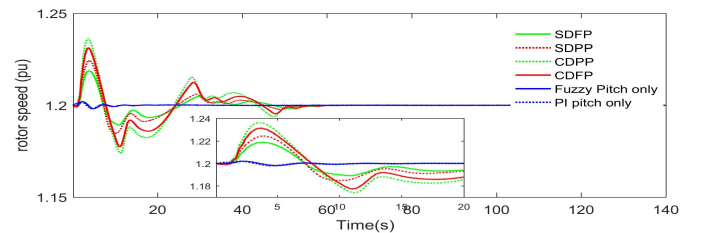


Fig. 21 DFIG rotor speed of wind farm A

The pitch angle with different control approaches as shown in Fig. 22 exhibit that SDFP outperforms other pitch angle controllers and also SDPP displays better pitch angle regulation than CDPP. The optimal regulation capability of SDFP through sectional droop and FLC pitch angle control demonstrates an optimal variation of DFIG active power output at wind farms A and B as shown in Fig. 23. Hence, the study reveals that the proposed SDFP is capable of providing similar level of superior performance than the conventional droop control and PI regulated pitch angle control.

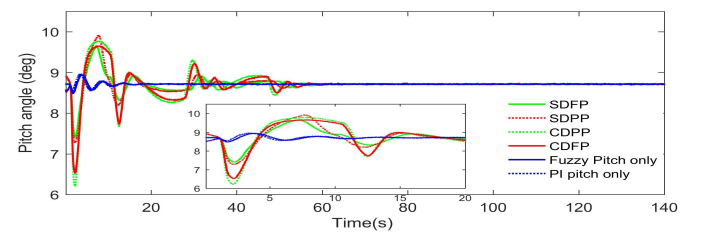


Fig. 22 The responses of DFIG pitch angle of wind farm A

In comparison to ES system which has the capability to provide prompt response, wind turbine does not have such ability due to its physical inertial properties. Therefore, the linear relation between power-frequency becomes a stress with high droop gain [51], especially close to low-frequency oscillations. Real-time simulation results substantiate that high droop gain during lower wind speed results large oscillations owing to the inertial nature of DFIG and may destabilize the system. Adopting a lower droop gain can be an alternative way of dealing with such large frequency oscillations. However, a lower droop gain will reduce the contribution of DFIG in PFC

which is undesirable from the stability perspective. Hence, there is a trade-off between the maximum DFIG contribution in PFC and the oscillation damping performance of the network with variable wind speed. However, with the proposed multi-gain droop control approach, such drawbacks can be overcome as this method reduces the droop gain during low-frequency deviations whereas the maximum PFC capability remains the same as in the conventional approach.

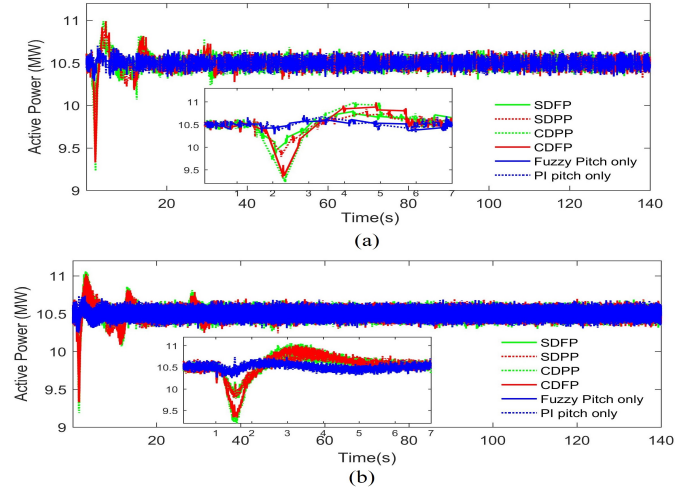


Fig. 23 Active power output of wind farm A (a) and B (b)

The proposed multi-gain droop demonstrates lower frequency oscillations when the deviation of grid frequency is small by reducing the droop gain in the low-frequency regions as shown in Figs. 9, 13, 16 and 20 through real-time simulation without compromising the maximum PFC contribution of DFIG as in the conventional droop control. It is shown in the above mentioned Figures that sectional droop control gain not only reduces the maximum and minimum frequency deviation but also demonstrates significant reduction in frequency oscillations over the simulation periods. Hence, it can be concluded that the proposed multi-gain droop control provides better performance than the conventional droop control. This observation illustrates that the better regulation capability of DFIG with lesser complexity in its control which can be more preferable choice for its industry application or academic field.

### 5.5. The Impact of Number Fuzzy Membership Functions on Frequency Performance

In order to evaluate the impact of various number of fuzzy membership functions on PFC, further real-time simulation studies have been carried out with 5 membership functions for both inputs and output of the fuzzy controller. The linguistic values are designated as Negative Big (NB), Negative Small (NS), Zero (ZE), Positive Small (PS) and Positive Big (PB). The membership functions for FLC inputs and output are shown in Fig. 24

For comparative analysis, the same load growth event of 5MW at Load A is applied for the duration of 1-1.45s. The dynamic frequency response with various membership functions are illustrated in Fig. 25. It can be seen that the

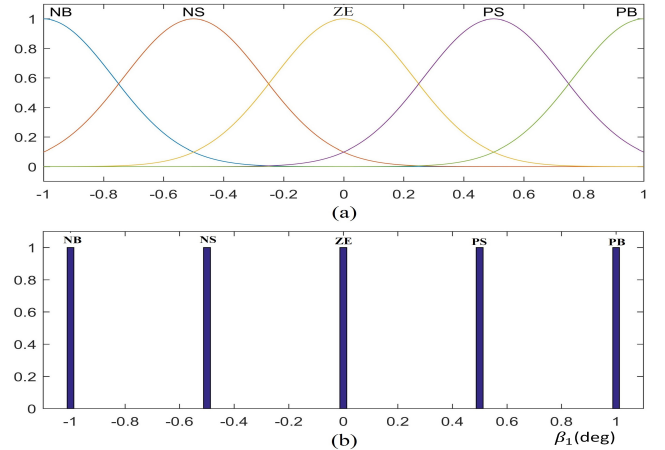


Fig. 24 FLC membership functions for (a) Rotor speed error and the integration of rotor speed error (b) pitch angle reference with 5 FLC membership functions

Table 6 FLC rules with 5 membership functions

$\int \Delta\omega_r$		NB	NS	ZE	PS	PB
$\Delta\omega_r$	NB	NB	NB	NS	NS	ZE
	NS	NB	NS	NS	ZE	PS
	ZE	NS	NS	ZE	PS	PS
	PS	NS	ZE	PS	PS	PB
	PB	ZE	PS	PS	PB	PB

number of membership functions has very little impact on the maximum and minimum frequency deviation values. However, as the time moves away from the disturbance point, FLC with 7 membership functions demonstrate better damping on the oscillation. The reason of such outcome is the fuzzy controller with 7 membership functions has  $7 \times 7 = 49$  rules and is capable of producing smoother output signal.

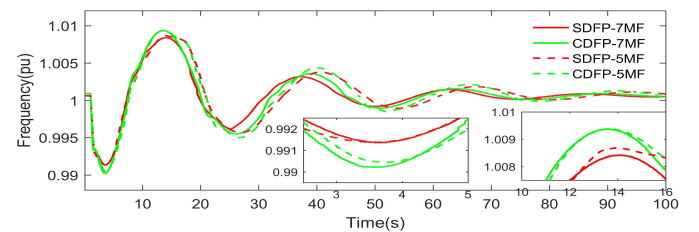


Fig. 25 The frequency outcome with different fuzzy membership functions

The improvements with 7 membership functions can further be observed in Figs. 26 and 27. Referring to both Figs., it can be seen that 7 membership functions manifest a moderately superior performance demonstrating better regulation of pitch angle and rotor speed mainly during low amplitude oscillations. This substantiates slightly the better accomplishment of fuzzy controller with higher membership functions and number of rules in frequency regulation. In conclusion, fuzzy controller with higher number of membership functions and rules can result in moderately better

performance. Nevertheless, computational complexity needs to be considered before selecting fuzzy controller with the large number of membership functions and rules for real-time implementation.

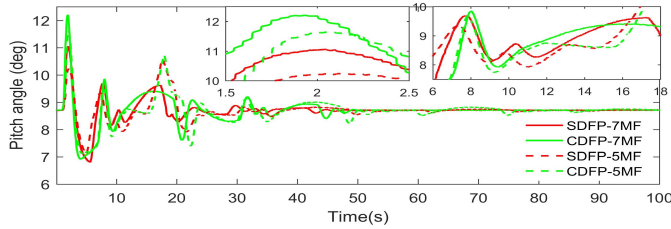


Fig. 26 The response of DFIG pitch angle with different fuzzy membership functions

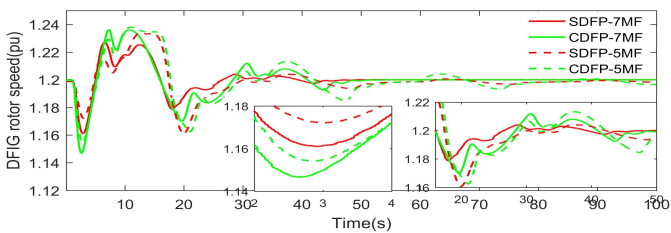


Fig. 27 The response of DFIG rotor speed with different fuzzy membership functions

## 6. Conclusion

In this paper, an integrated dynamic sectional droop control with inertia control for PFC regulation is proposed. The performance of the proposed coordinated controller is investigated with PI and FLC regulated pitch angle control to demonstrate the effectiveness of the control approach. The proposed dynamic sectional droop control is developed by dividing the conventional single P-f droop gain in two: low gain for lower frequency deviation and larger gain for the higher frequency deviation. The main findings of the proposed control approach through real-time simulation studies can be summarized as follows:

1. The proposed coordinated dynamic sectional droop (multi-gain) and inertia control manifests superior performance than the conventional fixed gain droop with both PI and FLC regulated pitch angle controllers. The sectional droop reduces frequency oscillations by lowering the P-f intensity when frequency deviation is small and vice versa.
2. The proposed control approach performs better with FLC regulated pitch angle control which reveals the dominance of FLC over traditional PI control method.
3. A high power margin for PFC results significant rise in frequency oscillation when wind speed is lower than the rated value and hence a lower power margin for PFC is applied when the wind speed is low.

4. The proposed sectional droop control with a higher or lower power margin at variable wind speed provides better performance than the conventional droop control. This demonstrates the flexibility of the proposed method for industry application which has minimum complexity yet processes robust performance capability.

**Conflicts of interest: None**

## Acknowledgment

The authors would like to thank OPAL-RT for the real time simulator OP5600 and associated trainings and the financial support provided by the Victoria University Research Training Program.

## References

### References

- [1] GWEC. Global Wind Report 2017, [Available Online]: <http://gwind.net/publications/global-wind-report-2/>, [Accessed on: 2018-10-25].
- [2] Li Y, Choi SS, Yang C, Wei F. Design of variable-speed dish-stirling solar-thermal power plant for maximum energy harness. *IEEE Transactions on Energy Conversion* 2015;301:394–403.
- [3] Zhang Y, Chen Z, Hu W, Cheng M. Flicker mitigation by individual pitch control of variable speed wind turbines with DFIG. *IEEE Transactions on Energy Conversion* 2014;291:20–28.
- [4] Troy N, Denny E, O'Malley M. Base-load cycling on a system with significant wind penetration. *IEEE Transactions on Power Systems* 2010;252:1088–1097.
- [5] Azzouz M, Elshafei A, Emara H. Evaluation of fuzzy-based maximum power-tracking in wind energy conversion systems. *IET Renewable Power Generation* 2011;56:422–430.
- [6] Sebastián R, Peña-Alzola R. Control and simulation of a flywheel energy storage for a wind diesel power system. *International Journal of Electrical Power & Energy Systems* 2015;64:1049 – 1056.
- [7] National Grid Electricity Transmission plc. The Grid Code, Issue 5, Revision 21, [Available Online]:<https://www.nationalgrid.com/sites/default/files/documents/8589935310-complete%20grid%20code.pdf>, [Accessed on: 2019-03-14].
- [8] IESO. Market Manual 2: Market Administration; Part 2.20: Performance Validation, [Available Online]:<http://www.ieso.ca/sector%20participants/market%20operations/-/media/84d0f4687aee4588ae13022aa29e31f7.ashx>, [Accessed on: 2019-03-14].
- [9] Energinet. Wind turbines connected to grids with voltages below 100 kV, [Available Online]:<https://en.energinet.dk/-/media/1196ee254b854d21ad88b2dc813bfea9.pdf?la=en&hash=acf6dbc39fef7340e206e48be4845941519cae97>, [Accessed on: 2019-03-14].
- [10] Energinet. Technical regulation 3.2.5 for wind power plants above 11 kW, [Available Online]:<https://en.energinet.dk/-/media/bd322e7805694462ab125e5b5d0d79bc.pdf?la=en&hash=db619e3ead98ad2f2691cea0b68be8b438f4b3fd>, [Accessed on: 2019-03-14].
- [11] EirGrid. EirGrid Grid Code, Version 6.0, [Available Online]:<http://www.eirgridgroup.com/site-files/library/eirgrid/gridcodeversion6.pdf>, [Accessed on: 2019-03-14].
- [12] TenneT GmbH . Requirements for Offshore Grid Connections in the Grid of TenneT TSO GmbH, [Available Online]:[https://www.tennet.eu/fileadmin/user\\_upload/the\\_electricity\\_market/german\\_market/grid\\_customers/tennet\\_tso\\_gmbh-asn-eng\\_21122012\\_final\\_1\\_.pdf](https://www.tennet.eu/fileadmin/user_upload/the_electricity_market/german_market/grid_customers/tennet_tso_gmbh-asn-eng_21122012_final_1_.pdf), [Accessed on: 2019-03-14].
- [13] GE Energy Applications and Systems Engineering. Technical Requirements for Wind Generation Interconnection and Integration , [Available Online]:[https://offshorewindhub.org/sites/default/files/resources/ge\\_11-3-2009\\_technologyforecasting\\_0.pdf](https://offshorewindhub.org/sites/default/files/resources/ge_11-3-2009_technologyforecasting_0.pdf), [Accessed on: 2019-03-14].

- [14] Australian Energy Market Operator. Hornsdale Wind Farm 2 FCAS trial , [Available Online]:<https://arena.gov.au/assets/2018/07/neoen-hornsdale-wind-farm-fcas-trial-report.pdf>, [Accessed on: 2019-03-14].
- [15] Zhang Y, Melin AM, Djouadi SM, Olama MM, Tomsovic K. Provision for guaranteed inertial response in diesel-wind systems via model reference control. *IEEE Transactions on Power Systems* 2018;336:6557–6568.
- [16] Liu F, Liu Z, Mei S, Wei W, Yao Y. Eso-based inertia emulation and rotor speed recovery control for DFIGs. *IEEE Transactions on Energy Conversion* 2017;323:1209–1219.
- [17] Gevorgian V, Zhang Y, Ela E. Investigating the impacts of wind generation participation in interconnection frequency response. *IEEE Transactions on Sustainable Energy* 2015;63:1004–1012.
- [18] Margaris ID, Papathanassiou SA, Hatziaegyriou ND, Hansen AD, Sorensen P. Frequency control in autonomous power systems with high wind power penetration. *IEEE Transactions on Sustainable Energy* 2012;32:189–199.
- [19] Vyver Jvd, Kooning JDMD, Meersman B, Vandeveld L, Vandoorn TL. Droop control as an alternative inertial response strategy for the synthetic inertia on wind turbines. *IEEE Transactions on Power Systems* 2016;312:1129–1138.
- [20] Tan Y, Meegahapola L, Muttaqi KM. A suboptimal power-point-tracking-based primary frequency response strategy for DFIGs in hybrid remote area power supply systems. *IEEE Transactions on Energy Conversion* 2016;311:93–105.
- [21] Wang Z, Wu W. Coordinated control method for DFIG-based wind farm to provide primary frequency regulation service. *IEEE Transactions on Power Systems* 2018;333:2644–2659.
- [22] Ghosh S, Kamalasan S, Senroy N, Enslin J. Doubly fed induction generator (DFIG)-based wind farm control framework for primary frequency and inertial response application. *IEEE Transactions on Power Systems* 2016;313:1861–1871.
- [23] Wang S, Hu J, Wang S, Tang H, Chi Y. Comparative study on primary frequency control schemes for variable-speed wind turbines. *The Journal of Engineering* 2017;201713:1332–1337.
- [24] Tian X, Wang W, Chi Y, Li Y, Liu C. Virtual inertia optimisation control of DFIG and assessment of equivalent inertia time constant of power grid. *IET Renewable Power Generation* 2018;1215:1733–1740.
- [25] Ochoa D, Martinez S. Fast-frequency response provided by DFIG-wind turbines and its impact on the grid. *IEEE Transactions on Power Systems* 2017;325:4002–4011.
- [26] Geng H, Xi X, Liu L, Yang G, Ma J. Hybrid modulated active damping control for DFIG-based wind farm participating in frequency response. *IEEE Transactions on Energy Conversion* 2017;323:1220–1230.
- [27] Baros S, Ilić MD. Distributed torque control of deloaded wind DFIGs for wind farm power output regulation. *IEEE Transactions on Power Systems* 2017;326:4590–4599.
- [28] Mahvash H, Taher SA, Rahimi M, Shahidehpour M. Enhancement of dfig performance at high wind speed using fractional order pi controller in pitch compensation loop. *International Journal of Electrical Power & Energy Systems* 2019;104:259 – 268.
- [29] Ibrahim AO, Nguyen TH, Lee D, Kim S. A fault ride-through technique of dfig wind turbine systems using dynamic voltage restorers. *IEEE Transactions on Energy Conversion* 2011;263:871–882.
- [30] Moradi H, Vossoughi G. Robust control of the variable speed wind turbines in the presence of uncertainties: A comparison between H-infinity and PID controllers. *Energy* 2015;90:1508 – 1521.
- [31] Kamel RM, Chaouachi A, Nagasaka K. Three control strategies to improve the microgrid transient dynamic response during isolated mode: A comparative study. *IEEE Transactions on Industrial Electronics* 2013;604:1314–1322.
- [32] Civelek Z, Lüy M, Çam E, Mamur H. A new fuzzy logic proportional controller approach applied to individual pitch angle for wind turbine load mitigation. *Renewable Energy* 2017;111:708 – 717.
- [33] Boëda D, Teninge A, Roye D, Bacha S, Belhomme R. Contribution of wind farms to frequency control and network stability. *European Wind Energy Conference (EWEC), 2007*, p. 1–10.
- [34] Teninge A, Jecu C, Roye D, Bacha S, Duval J, Belhomme R. Contribution to frequency control through wind turbine inertial energy storage. *IET Renewable Power Generation* 2009;33:358–370.
- [35] Oh KY, Park JY, Lee JS, Lee J. Implementation of a torque and a collective pitch controller in a wind turbine simulator to characterize the dynamics at three control regions. *Renewable Energy* 2015;79:150 – 160.
- [36] Zhang Z, Sun Y, Lin J, Li G. Coordinated frequency regulation by doubly fed induction generator-based wind power plants. *IET Renewable Power Generation* 2012;61:38–47.
- [37] Gholamrezaie V, Dozein MG, Monsef H, Wu B. An optimal frequency control method through a dynamic load frequency control (LFC) model incorporating wind farm. *IEEE Systems Journal* 2018;121:392–401.
- [38] Arani MFM, Mohamed YAI. Analysis and impacts of implementing droop control in DFIG-based wind turbines on microgrid/weak-grid stability. *IEEE Transactions on Power Systems* 2015;301:385–396.
- [39] Chamorro HR, Riaño I, Gerndt R, Zelinka I, Gonzalez-Longatt F, Sood VK. Synthetic inertia control based on fuzzy adaptive differential evolution. *International Journal of Electrical Power & Energy Systems* 2019;105:803 – 813.
- [40] Penga B, Zhanga F, Lianga J, Dinga L, Liangb Z, Wu Q. Coordinated control strategy for the short-term frequency response of a dfig-es system based on wind speed zone classification and fuzzy logic control. *International Journal of Electrical Power & Energy Systems* 2019;107:363–378.
- [41] Hwang M, Muljadi E, Park J, Sørensen P, Kang YC. Dynamic droop-based inertial control of a doubly-fed induction generator. *IEEE Transactions on Sustainable Energy* 2016;73:924–933.
- [42] Vidyandandan KV, Senroy N. Primary frequency regulation by deloaded wind turbines using variable droop. *IEEE Transactions on Power Systems* 2013;282:837–846.
- [43] Fu Y, Zhang X, Hei Y, Wang H. Active participation of variable speed wind turbine in inertial and primary frequency regulations. *Electric Power Systems Research* 2017;147:174 – 184.
- [44] Zhao J, Lyu X, Fu Y, Hu X, Li F. Coordinated microgrid frequency regulation based on DFIG variable coefficient using virtual inertia and primary frequency control. *IEEE Transactions on Energy Conversion* 2016;313:833–845.
- [45] Wu YK, Yang WH, Hu YL, Dzung PQ. Frequency regulation at a wind farm using time-varying inertia and droop controls. *IEEE Transaction on Industry Application* 2019;551:213–224.
- [46] Garmroodi M, Verbič G, Hill DJ. Frequency support from wind turbine generators with a time-variable droop characteristic. *IEEE Transactions on Sustainable Energy* 2018;92:676–684.
- [47] Li P, Hu W, Hu R, Huang Q, Yao J, Chen Z. Strategy for wind power plant contribution to frequency control under variable wind speed. *Renewable Energy* 2019;130:1226–1236.
- [48] Zhu X, Xia M, Chiang HD. Coordinated sectional droop charging control for EV aggregator enhancing frequency stability of microgrid with high penetration of renewable energy sources. *Applied Energy* 2018;210:936 – 943.
- [49] Pradhan C, Bhende CN, Samanta AK. Adaptive virtual inertia-based frequency regulation in wind power systems. *Renewable Energy* 2018;115:558–574.
- [50] Lee J, Muljadi E, Sørensen P, Kang Y. Releasable kinetic energy-based inertial control of a dfig wind power plant. *IEEE Transaction Sustainable Energy* 2016;71:279–288.
- [51] Arani MFM, Mohamed YAI. Dynamic droop control for wind turbines participating in primary frequency regulation in microgrids. *IEEE Transaction on Smart Grid* 2018;96:5742–5751.
- [52] Tao C, Taur J, Chang Y, Chang C. A novel fuzzy-sliding and fuzzy-integral-sliding controller for the twin-rotor multi-input–multi-output system. *IEEE Transactions on Fuzzy Systems* 2010;185:893–905. doi : 10.1109/TFUZZ.2010.2051447.
- [53] Chen J, Chen J, Gong C. New overall power control strategy for variable-speed fixed-pitch wind turbines within the whole wind velocity range. *IEEE Transactions on Industrial Electronics* 2013;607:2652–2660. doi : 10.1109/TIE.2012.2196901.